ISSN 1054-660X, Laser Physics, 2007, Vol. 17, No. 2, pp. 174–179.

Transverse Effects in Collective Atomic Recoil Lasing

N. Piovella, L. Volpe, M. M. Cola, and R. Bonifacio

Dipartimento di Fisica, Università Degli Studi di Milano and INFN, Via Celoria 16, I-20133 Milano, Italy

e-mail: nicola.piovella@mi.infn.it

Received July 27, 2006

Abstract—We investigate transverse effects in collective atomic recoil lasing (CARL), where a cold atomic sample is lightened by a far detuned laser beam resonant with the internal atomic transition. The gradient force of the scattered radiation field produces a collective self-focusing on the atoms, which could be observed in a Bose–Einstein condensate stored in a bidirectional optical ring cavity or in the superradiant CARL–BEC regime.

PACS numbers: 42.50.Vk, 42.50.Fx, 03.75.Kk

DOI: 10.1134/S1054660X07020223

1. INTRODUCTION

The realization of Bose–Einstein Condensates (BEC) of dilute alkali gases [1, 2] has made it possible to study new collective effects in the interaction between light and atoms prepared in a single quantum state. Among them, collective light scattering by coherent center-of-mass motion of atoms in a condensate illuminated by a far off-resonant laser has been recently observed [3–7] and interpreted as superradiant collective atomic recoil lasing (CARL [8]) in the quantum regime [9–13]. Using a BEC, the quantum CARL is described by a Gross–Pitaevskii model generalized to include the self-consistent evolution of the scattered radiation amplitude [7].

Until now, the model has been developed only for the longitudinal dimension of a cigar-shaped condensate. In this paper, we extend the previous 1D model to include the transverse dynamics of the atoms and the scattered field. We find a new self-focusing effect on the atoms due to the collective scattering process, of which a preliminary description is here reported.

2. TRANSVERSE EFFECTS IN CARL AND CLASSICAL SELF-FOCUSING FORCE

We start from the CARL Hamiltonian [8]

$$H = \frac{1}{2m}(p_\perp^2 + p_z^2) - i\hbar\frac{g_1}{2\Delta_0}\{\Omega_p^* a e^{2ikz} - \text{c.c.}\} + \hbar\frac{|\Omega_p|^2}{4\Delta_0}, \quad (1)$$

which describes the interaction of a two-level atom with two counterpropagating fields along the $\hat{z}$ axis, i.e., a pump laser with Rabi frequency $\Omega_p = dE_p/\hbar$ and frequency ω_p, and a self-consistent back-scattered field with frequency $\omega = \omega_p - \Delta_r$ and classical amplitude $a = (\epsilon_0 V/2\hbar\omega)^{1/2}E$ evolving according to the paraxial Maxwell equation:

$$\left(\frac{\partial}{\partial t} + c\frac{\partial}{\partial z}\right)a + \frac{c}{2ik}\nabla_\perp^2 a = \frac{g_1\Omega_p^*}{2\Delta_0}N\langle e^{-2ikz}\rangle + i\Delta_r a, \quad (2)$$

where $k = \omega/c$, N is the number of atoms, $g_1 = d[\omega/(2\hbar\epsilon_0 V)]^{1/2}$ is the electric dipole coupling constant, d is the atomic dipole moment, m is the atomic mass, V is the mode volume, and $\langle e^{-2ikz}\rangle$ is the local longitudinal bunching. The pump laser is far detuned from the atomic resonance ω_0; i.e., $\Delta_0 = \omega - \omega_0$ is much larger than the natural linewidth of the atomic transition. If the pump field Ω_p is constant and uniform, the last term in (1) can be neglected and, defining $g = g_1\Omega_p/2|\Delta_0|$, Eqs. (1) and (2) become

$$H = \frac{1}{2m}(p_\perp^2 + p_z^2) - i\hbar g\{a e^{i\theta} - \text{c.c.}\}, \quad (3)$$

$$\left(\frac{\partial}{\partial t} + c\frac{\partial}{\partial z}\right)a + \frac{c}{2ik}\nabla_\perp^2 a = gN\langle e^{-i\theta}\rangle + i\Delta_r a, \quad (4)$$

where $\theta = 2kz$ and we have assumed Ω_p real. If the atomic sample has a transverse profile, then the scattered field amplitude a grows initially with the same profile of the atomic sample. This transverse spatial dependence in a originates a mean gradient self-force on the atoms

$$\frac{d\langle \mathbf{p}_\perp\rangle}{dt} = -\langle \nabla_\perp H\rangle = i\hbar g[(\nabla_\perp a)\langle e^{i\theta}\rangle - \text{c.c.}] \quad (5)$$

which is proportional to the longitudinal bunching $b = \langle e^{-i\theta}\rangle$ and whose sign depends on the bunching phase. Notice that the average $\langle\ldots\rangle$ in (4) and (5) is on θ only, i.e., on the fast scale $\Delta z = \lambda/2$.

To give a rough description of this focusing force, let us suppose that the relevant dependence on the transverse coordinate in the scattered field is on the

intensity rather than on the phase. Hence, writing $a = |a|e^{i\phi}$, we have from Eq. (5)

$$\frac{d\langle \mathbf{p}_\perp \rangle}{dt} \approx -2\hbar g \langle \sin(\theta + \phi)\rangle \nabla_\perp |a|. \quad (6)$$

Since in general $\nabla_\perp |a| < 0$ (the atomic transverse profile decreases away from the $\hat{z}$ axis), the interplay between photon emission and atomic bunching induces a self-focusing only when $\langle \sin(\theta + \phi)\rangle < 0$. Neglecting radiation diffraction and propagation, Eq. (4) yields

$$gN\langle \sin(\theta + \phi)\rangle \approx -(\dot{\phi} - \Delta_r)|a|, \quad (7)$$

where $\dot{\phi} = d\phi/dt$. Inserting this into (6), we have

$$\frac{d\langle \mathbf{p}_\perp \rangle}{dt} \approx \hbar(\dot{\phi} - \Delta_r)(\nabla_\perp |a|^2/N). \quad (8)$$

Hence, the scattered radiation induces a self-focusing force when $\dot{\phi} > \Delta_r$. In the 1D classical evolution of CARL, this results in $\dot{\phi} > 0$ for $\Delta_r = 0$ [8], so that some self-focusing is expected to occur when the transverse profile of the scattered intensity is sufficiently steep. In order to give a rough estimate of this self-focusing in the classical regime of CARL, we assume, for $\Delta_r = 0$, a maximum intensity and phase shift of the scattered radiation given by $|a|^2_{\max} \sim \rho N$ and $\dot{\phi} \sim \omega_r \rho$, respectively, where $\omega_r = (2\hbar k)^2/2m$ is the recoil frequency and $\rho = (g\sqrt{2N}/\omega_r)^{2/3}$ is the CARL parameter [8]. Furthermore, we assume along the transverse direction x, $\partial_x |a|^2 \sim -(x/\sigma^2)|a|^2$, where σ is the transverse section of the atomic sample, so that from Eq. (8) we obtain $\ddot{x} \approx -\omega^2_{\rm foc} x$, where $\omega_{\rm foc} = [\hbar\omega_r\rho^2/(m\sigma^2)]^{1/2}$ and the characteristic focusing time is approximately $\tau_{\rm foc} \sim 1/\omega_{\rm foc}$. Assuming for instance a cold sample of ^{87}Rb atoms illuminated by a pump laser at $\lambda = 780$ nm, then $\omega_r \sim 10^5$ s^{-1} and $g \sim 10^7 I_0^{1/2}/|\Delta_0|$ s^{-1}, where I_0 is the pump intensity in mW/cm^2 and Δ_0 is the pump–atom detuning in megahertz. Using these values, $\tau_{\rm foc} \sim 3\sigma(\Delta_0^2/NI_0)^{1/3}$ μs, where σ is in micrometers. For instance, for $N \sim 10^6$, $I_0 \sim 100$ mW/cm^2, $\Delta_0 \sim 1$ THz and $\sigma \sim 10$ μm, we have $\tau_{\rm foc} \sim 600$ μs. Hence, the self-focusing force could be observable in a typical CARL experiment with cold atoms in an optical high-finesse ring cavity [14].

In the rest of the paper, we investigate the self-focusing in the quantum CARL regime, where the atomic sample is a Bose–Einstein condensate, discussing the "good-cavity" and the superradiant regimes.

3. SELF-FOCUSING IN CARL–BEC

The quantum model for the matter wave field $\Psi(\mathbf{x}_\perp, \theta, t)$ and the radiation field $a(\mathbf{x}_\perp, \theta, t)$ [7, 10], extended to include the transverse dynamics of the atoms and the radiation, is

$$i\frac{\partial \Psi}{\partial t} = (H/\hbar)\Psi = -\frac{\hbar}{2m}\nabla_\perp^2\Psi - \omega_r\frac{\partial^2}{\partial\theta^2}\Psi - ig(ae^{i\theta} - \text{c.c.})\Psi, \quad (9)$$

$$\left(\frac{\partial}{\partial t} + 2\omega\frac{\partial}{\partial\theta}\right)a + \frac{c}{2ik}\nabla_\perp^2 a = gN|\Psi(\theta, \mathbf{x}, t)|^2 e^{-i\theta} + i\Delta_r a, \quad (10)$$

where $\Psi(\theta, \mathbf{x}_\perp, t)$ is normalized to unity, i.e.,

$$\int_0^{2\pi} d\theta \int d^2\mathbf{x}_\perp |\Psi(\theta, \mathbf{x}_\perp, t)|^2 = 1. \quad (11)$$

In Eq. (9), we have neglected the nonlinear term describing the atom–atom interaction, which eventually can be straightforwardly included in a future analysis. Using the "mean field" approximation for the radiation field and scaling the transverse coordinates in units of the transverse section σ of the condensate, i.e., $x' = x/\sigma$, Eqs. (9) and (10) become

$$i\frac{\partial \Psi}{\partial t} = -\left[\omega_\perp \nabla^2_{x'} + \omega_r\frac{\partial^2}{\partial\theta^2}\right]\Psi - ig(ae^{i\theta} - \text{c.c.})\Psi, \quad (12)$$

$$\frac{\partial a}{\partial t} - i\frac{c}{Z_R}\nabla^2_{x'}a = gN\int_0^{2\pi} d\theta |\Psi(\theta, \mathbf{x}', t)|^2 e^{-i\theta} + (i\Delta_r - \kappa_c)a. \quad (13)$$

Here, κ_c is the radiation damping (equal to $cT/L_{\rm cav}$ in a ring cavity of length $L_{\rm cav}$ and mirror transmissivity T, or approximately equal to c/L in free space, where L is the condensate length); $\omega_\perp = \hbar/2m\sigma^2 = E_\perp/\hbar$ is the transverse frequency, where $E_\perp = \sigma^2_{p_\perp}/2m$ and $\sigma_{p_\perp} = \hbar/\sigma$; and $Z_R = 4\pi\sigma^2/\lambda$ is the Rayleigh range of the optical field, with a minimum spot size of $w_0 = 2\sigma$.

Expanding $\Psi(\theta, \mathbf{x}_\perp, t)$ in the Fourier series on θ,

$$\Psi(\theta, \mathbf{x}', t) = \frac{1}{\sqrt{2\pi}}\sum_{n=-\infty}^{\infty} c_n(\mathbf{x}', t)e^{in(\theta + \Delta_r t)}, \quad (14)$$

and defining $a = \bar{a}e^{i\Delta_r t}$, we transform Eqs. (12) and (13) to

$$\frac{\partial c_n}{\partial t} = -in(n\omega_r + \Delta_r)c_n + i\omega_\perp\nabla^2_{x'}c_n - g[\bar{a}c_{n-1} - \bar{a}^* c_{n+1}], \quad (15)$$

$$\frac{\partial \bar{a}}{\partial t} - i\frac{c}{Z_R}\nabla^2_{x'}\bar{a} = gN\sum_{n=-\infty}^{\infty} c^*_{n-1}c_n - \kappa_c\bar{a}. \quad (16)$$

Let us now assume the "two-level" approximation, in which the atoms change their momentum state only from the initial value $p = 0$ (i.e., $n = 0$) to the recoiled momentum $p = -2\hbar k$ (i.e., $n = -1$) [9–11]. In this regime, the momentum states with $n \neq 0, -1$ remain approximately empty, so that the Hilbert space is spanned by only the two states $|0\rangle$ and $|-1\rangle$ and Eqs. (15) and (16) reduce to

$$\frac{\partial c_0}{\partial t} = i\omega_\perp\nabla^2_{x'}c_0 - g\bar{a}c_{-1}, \quad (17)$$

$$\frac{\partial c_{-1}}{\partial t} = i(\Delta_r - \omega_r)c_{-1} + i\omega_\perp\nabla^2_{x'}c_{-1} + g\bar{a}^*c_0, \quad (18)$$

$$\frac{\partial \bar{a}}{\partial t} - i\frac{c}{Z_R}\nabla^2_{x'}\bar{a} = gNc^*_{-1}c_0 - \kappa_c\bar{a}. \quad (19)$$

Finally, introducing the scaled time $\bar{t} = (g\sqrt{N})t$ and the field amplitude $A = \bar{a}/\sqrt{N}$, Eqs. (17)–(19) become

$$\frac{\partial c_0}{\partial \bar{t}} = i\eta\nabla^2_{x'}c_0 - Ac_{-1}, \quad (20)$$

$$\frac{\partial c_{-1}}{\partial \bar{t}} = i\Delta c_{-1} + i\eta\nabla^2_{x'}c_{-1} + A^*c_0, \quad (21)$$

$$\frac{\partial A}{\partial \bar{t}} - iD\nabla^2_{x'}A = c_0c^*_{-1} - \kappa A, \quad (22)$$

where $\Delta = (\Delta_r - \omega_r)/g\sqrt{N}$,

$$\kappa = \frac{\kappa_c}{g\sqrt{N}}, \quad \eta = \frac{\omega_\perp}{g\sqrt{N}}, \quad D = \frac{c}{Z_R g\sqrt{N}} = \frac{c}{v_r}\eta, \quad (23)$$

where $v_r = \hbar k/m$ is the recoil velocity. We recall that, in the good cavity regime ($\kappa_c \ll g\sqrt{N}$, i.e., $\kappa \ll 1$), the "two-state" approximation is valid when $\omega_r > g\sqrt{N}$ [10]. On the other hand, in the superradiant regime ($\kappa_c \geq g\sqrt{N}$, i.e., $\kappa \geq 1$), the "two-state" approximation is valid when $\omega_r > g^2N/\kappa_c = G$, where G is the superradiant gain [10, 13].

4. ANALYSIS

We have numerically solved Eqs. (20)–(22) considering for simplicity a single transverse coordinate x'. We assumed as initial conditions $A(x', 0) = 0$, $c_0(x', 0) = \sqrt{n_0(x')}$ and $c_{-1}(x', 0) = b_0\sqrt{n_0(x')}$, where $n_0(x')$ is the initial transverse profile of the condensate and $b_0 = \langle e^{-i\theta}\rangle_0$ is the average initial hunching. In all the simulations, we assumed resonance ($\Delta = 0$) and $b_0 = 10^{-3}$. Note that Eqs. (20)–(22) depend on three dimensionless parameters: η, D, and κ. We have investigated the atomic self-focusing separately for the good-cavity regime (with $\kappa \ll 1$) and for the superradiant regime (with $\kappa \geq 1$).

4.1. Good-Cavity Regime $\kappa \ll 1$

If the condensate is inserted in the mode volume of a high-finesse optical ring cavity, we may assume $\kappa = 0$ in Eqs. (20)–(22). In order to observe the self-focusing effect alone, we have initially solved Eqs. (20)–(22) neglecting also diffraction, i.e., for $D = 0$. The numerical analysis shows self-focusing for $\eta \simeq 0.01$–0.10. As an example, Fig. 1 shows the radiated energy $E = \int dx|A|^2$ (a) and the condensate profile (b–d) $n = |c_0|^2 + |c_{-1}|^2$ at different times for $\eta = 0.1$. The initial atomic transverse profile is a Gaussian (dashed line in Fig. 1b–1d). We observe that, during the exponential build up of the radiation intensity (Fig. 1b), the atoms diffract, whereas they focus toward the center after the radiation intensity has reached the first peak (see Fig. 1c, 1d). Here, the condensate develops two transverse wings which move away from the axis due to atomic diffraction, whereas the central core of the condensate strongly focus near the center. This behavior is more evident from the color maps of Figs. 2 and 3, where the evolution of the radiation intensity $|A(x', \bar{t})|^2$ and the condensate density $n(x', \bar{t})$ is shown.

A preliminary numerical analysis shows that atomic self-focusing seems not to be strongly affected by radiation diffraction, as can be seen in Fig. 4, showing n for $\eta = 0.02$, $D = 10\eta$, and $\kappa = 0$. Conversely, self-focusing also disappears for modest values of κ, as shown in Fig. 5 for $\eta = 0.02$, $D = 0$, and $\kappa = 10\eta$: here the condensate diffracts for $\bar{t} > 30$, after the emission of a first burst of radiation (not shown in the figure). At later times, the atomic density is too small to stimulate further emission of photons.

4.2. Superradiant Regime $\kappa \geq 1$

In the superradiant (or superfluorescence (SF) [15]) regime, no optical cavity is assumed, so that usually $\kappa \gg 1$ [10, 13]. This regime corresponds to the recent experiments of [3–7], in which the atoms have been seen to move monotonically from the initial momentum state $p = 0$ to the recoiling state $p = -2\hbar k$ after emission of a short superradiant burst of radiation in the direction opposite to the pump laser. In the SF, radiation diffraction is negligible for a large Fresnel number $F = Z_R/L \gg 1$ [16, 17], i.e., for $\kappa \gg D$. In this regime, Eq. (22) can be solved in the adiabatic approximation,

$$A \approx \frac{1}{\kappa}c_0c^*_{-1}, \quad (24)$$

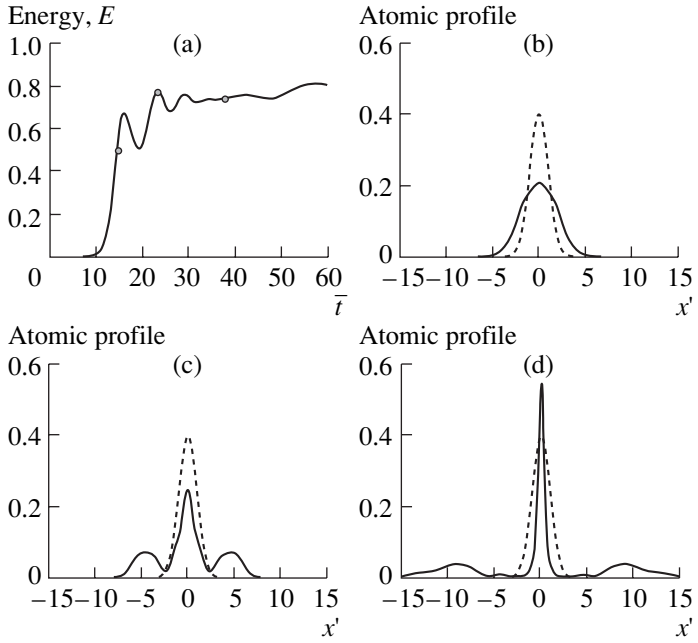

Fig. 1. Good-cavity regime, $\kappa = 0$, and no diffraction, $D = 0$, for $\eta = 0.1$. Total energy E (a) vs. $\bar{t}$ and transverse profile of the condensate vs. $x' = x/\sigma$ at $\bar{t} = 15$ (b), 23.4 (c), and 38 (d), for an initial Gaussian profile (dashed line).

and inserted in (20) and (21) to yield

$$\frac{\partial c_0}{\partial \bar{t}} = i\eta\nabla^2_{x'}c_0 - \frac{1}{\kappa}|c_{-1}|^2 c_0, \tag{25}$$

$$\frac{\partial c_{-1}}{\partial \bar{t}} = i\Delta c_{-1} + i\eta\nabla^2_{x'}c_{-1} + \frac{1}{\kappa}|c_0|^2 c_{-1}. \tag{26}$$

Defining $t' = \bar{t}/\bar{\kappa} = Gt$ and $\Delta' = \kappa\Delta = (\Delta_r - \omega_r)/G$ (where $G = g^2N/\kappa_c$ is the superradiant gain), Eqs. (25)–(26) become

$$\frac{\partial c_0}{\partial t'} = i\eta'\nabla^2_{x'}c_0 - |c_{-1}|^2 c_0, \tag{27}$$

$$\frac{\partial c_{-1}}{\partial t'} = i\eta'\nabla^2_{x'}c_{-1} + i\Delta' c_{-1} + |c_0|^2 c_{-1}, \tag{28}$$

where

$$\eta' = \kappa\eta = \frac{\omega_\perp}{G}. \tag{29}$$

We have numerically integrated the reduced Eqs. (27) and (28) for several values of η' and $\Delta' = 0$. As an example, Fig. 6 shows the radiation energy E vs. t' (Fig. 6a) and the density profile n vs. x' (Fig. 6b) at $t' = 0$ (dashed line) and $t' = 25$ (continuous line), for $\eta' = 0.005$. We found that, in the superradiant regime, the self-focusing effect is much more reduced than the one observed in the "good-cavity regime," although a weak focusing in the central core of the condensate is still visible, as shown by Fig. 6b. In these simulations, we assumed a flat-top profile (dashed line in Figs. 6b and 7b) in order to increase the profile steepness and so the gradient force.

As a last example of superradiance, we have considered a case with a Fresnel number $F = 1$ (i.e., $\kappa = D$) and $\eta = 0.002$. Figure 7 shows the radiation energy E vs. t' (a) and the density profile n vs. x' (b) at $t' = 0$ (dashed line) and $t' = 100$ (continuous line). We still observe some atomic focusing but without side wings.

5. DISCUSSION

Typical experimental values (see [13] and references therein) for a ^{87}Rb condensate illuminated by a pump beam of wavelength $\lambda = 780$ nm are $\omega_r \sim 10^5$ s^{-1}, $g \sim 10^7 I_0^{1/2}/|\Delta_0|$ s^{-1}, and $\omega_\perp \sim 360/\sigma^2$ s^{-1}, where I_0 is in mW/cm^2, Δ_0 is in megahertz, and σ is in micrometers.

Let us first consider the "good-cavity" regime, with $\kappa = 0$. Since it must be $\omega_r \geq g\sqrt{N}$, this implies $\Delta_0/\sqrt{I_0 N} > 10^2$. Assuming $N \sim 10^5$, $\Delta_0 = 1$ THz, and $I_0 = 10$ mW/cm^2, then $g\sqrt{N} \sim 10^4$ s^{-1}. Since $\eta \sim 4 \times 10^{-2}/\sigma^2$, in order to have $\eta > 0.01$, we needs $\sigma < 2$ μm, as for instance those recently produced in microtraps [18]. However, in a typical optical ring cavity, the transverse section of the cavity mode is usually much larger than the condensate section, so that it is rather unrealistic to neglect radiation diffraction assuming $D = 0$. Instead, a more realistic behavior could be the one shown in Fig. 4, where $D \gg \eta$.

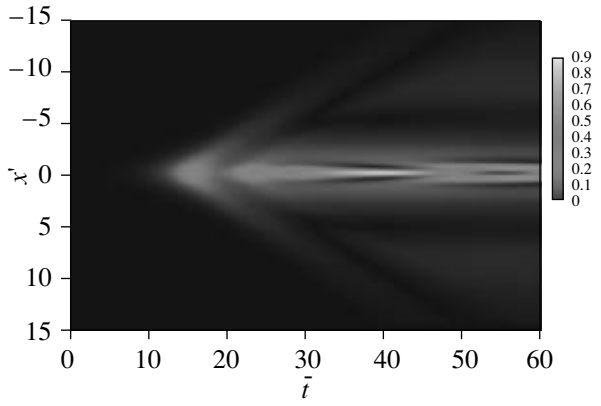

Fig. 2. Transverse profile $|A|^2$ of the radiation intensity vs. x' and $\bar{t}$, for $\eta = 0.1$, $\kappa = 0$, and $D = 0$.

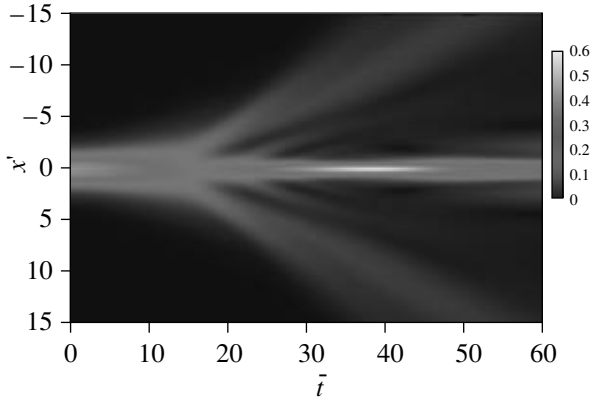

Fig. 3. Transverse density n of the condensate vs. x' and $\bar{t}$, for $\eta = 0.1$, $\kappa = 0$, and $D = 0$.

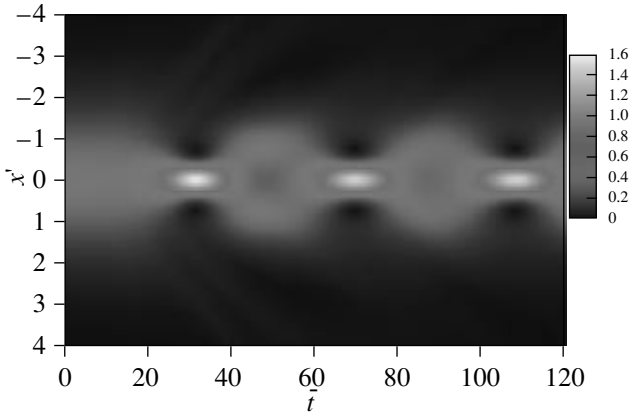

Fig. 4. Transverse density $n(x', \bar{t})$ of the condensate vs. x' and $\bar{t}$ for $\eta = 0.02$, $D = 10\eta$, and $\kappa = 0$.

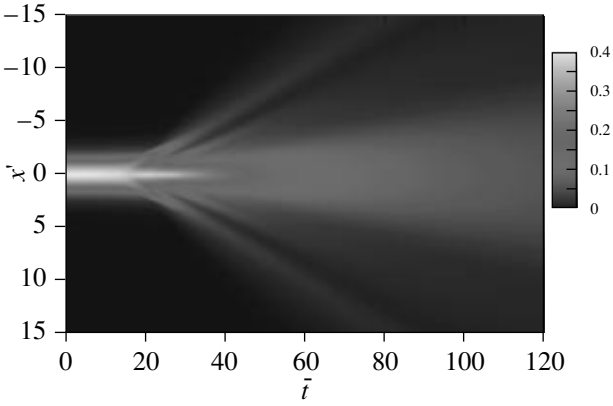

Fig. 5. Transverse density $n(x', \bar{t})$ of the condensate vs. x' and $\bar{t}$ for $\eta = 0.02$, $D = 0$, and $\kappa = 0.2$.

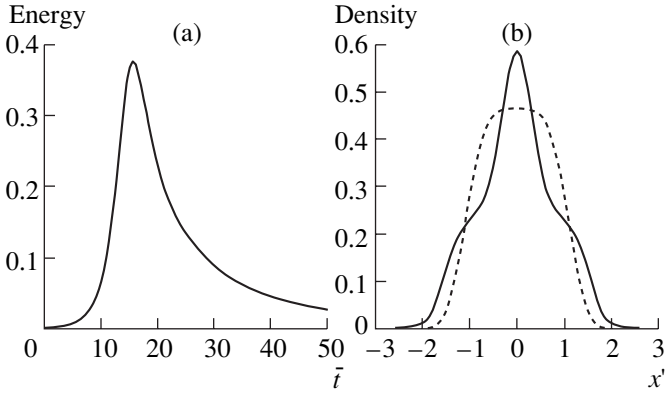

Fig. 6. Superradiant regime for $\eta' = 0.005$. Total energy E (a) vs. $\bar{t}$ and atomic transverse profile n vs. $x' = x/\sigma$ (b) at $t' = 25$ (continuous line) for a flat-top initial profile (dashed line).

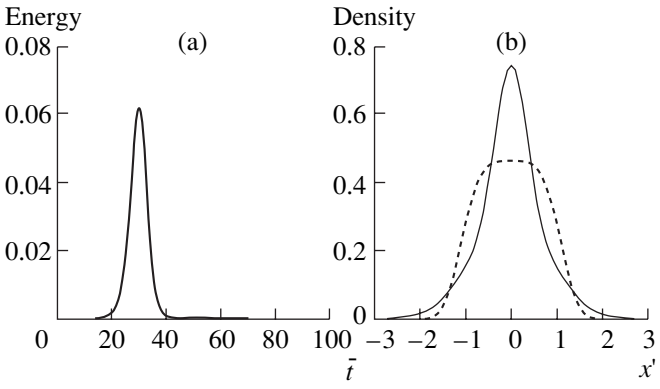

Fig. 7. Superradiant regime for $\eta' = 0.002$ and $\kappa = D = 1$. Total energy E (a) vs. $\bar{t}$ and atomic transverse profile n vs. $x' = x/\sigma$ (b) at $\bar{t} = 100$ (continuous line) for a flat-top initial profile (dashed line).

In the superradiant regime [3–7], there is no optical cavity, so that $\kappa_c \sim c/L \sim 3 \times 10^{14}/L$ s^{-1}, where L is the condensate length in micrometers. Since it must be $\omega_r \geq G$, this imposes the condition $\Delta_0^2/(NLI_0) > 10^{-5}$. In previous experiments, (see, for instance, [13]), $N \sim 10^5$, $\Delta_0 \sim 1$ GHz, $I_0 \sim 100$ mW/cm^2, $L \sim 100$ μm, and $\sigma \sim 10$ μm, so that $G \sim 10^4$ s^{-1}. Since $Z_R \gg L$, radiation diffraction is negligible and the relevant parameter for atomic focusing is $\eta' = \omega_\perp/G \sim 10^{-4}$, so that self-focusing was negligible in these experiments. However, decreasing the pump intensity by a factor 10 should be enough to reproduce the case of Fig. 6, with some focusing observed after some milliseconds of exposition to the pump laser.

6. CONCLUSIONS

We have shown a new self-focusing effect in the collective atomic recoil lasing (CARL), which could be observed by a proper choice of the parameters in the recent experiments on CARL superradiance with BECs. Also, self-focusing effects should be more likely observable in a future experiment where the condensate is positioned in a high-finesse optical ring cavity [19]. Note that similar self-focusing effects have also been predicted in [20], but in the Thomas–Fermi limit, i.e., when the atomic kinetic energy is negligible with respect to the mean-field energy of the condensate.

REFERENCES

1. M. H. Anderson, J. R. Ensher, M. R. Matthews, et al., Science **269**, 198 (1995).
2. Ph. W. Courteille, V. S. Bagnato, and V. I. Yukalov, Laser Phys. **11**, 659 (2001).
3. S. Inouye, A. P. Chikkatur, D. M. Stamper-Kurn, et al., Science **285**, 571 (1999).
4. S. Inouye, T. Pfau, S. Gupta, et al., Nature **402**, 641 (1999).
5. M. Kozuma, Y. Suzuki, Y. Torii, et al., Science **286**, 2309 (1999).
6. D. Schneble, Y. Torii, M. Boyd, et al., Science **300**, 475 (2003).
7. L. Fallani, C. Fort, N. Piovella, et al., Phys. Rev. A **71**, 033612 (2005).
8. R. Bonifacio and L. De Salvo Souza, Nucl. Instrum. Methods Phys. Res. A **341**, 360 (1994); R. Bonifacio, L. De Salvo Souza, L. Narducci and E.J. D'Angelo, Phys. Rev. A **50**, 1716 (1994).
9. M. G. Moore and P. Meystre, Phys. Rev. A **58**, 3248 (1998); M. G. Moore, O. Zobay, and P. Meystre, Phys. Rev. A **60**, 1491 (1999).
10. N. Piovella, M. Gatelli, and R. Bonifacio, Opt. Comm. **194**, 167 (2001).
11. N. Piovella, M. Cola, and R. Bonifacio, Phys. Rev. A **67**, 013817 (2003).
12. M. M. Cola and N. Piovella, Phys. Rev. A **70**, 043809 (2004).
13. G. R. M. Robb, N. Piovella, and R. Bonifacio, J. Opt. B: Quantum Semiclass. Opt. **7**, 93 (2005).
14. D. Kruse, C. von Cube, C. Zimmermann, and P. W. Courteille, Phys. Rev. Lett. **91**, 183601 (2003); C. von Cube, et al., Phys. Rev. Lett. **93**, 083601 (2004).
15. R. Bonifacio and L. A. Lugiato, Phys. Rev. A **11**, 1507 (1975).
16. R. Bonifacio, J. D. Farina, and L. M. Narducci, Opt. Comm. **31**, 377 (1979).
17. F. P. Mattar, H. M. Gibbs, S. L. McCall, and M. S. Feld, Phys. Rev. Lett. **46**, 1123 (1981).
18. J. Fortàgh, et al., Opt. Commun. **243**, 45 (2004).
19. P. Courteille, private communication.
20. S. Giovanazzi, D. O'Dell, and G. Kurizki, Phys. Rev. Lett. **88**, 130402 (2002).